Plant Physiology®

A digital sensor to measure real-time leaf movements and detect abiotic stress in plants

Batist Geldhof [ID],[1] Jolien Pattyn [ID],[1] David Eyland [ID],[2] Sebastien Carpentier [ID],[2,3] and Bram Van de Poel [ID][1,*,†]

1 Department of Biosystems, Division of Crop Biotechnics, Molecular Plant Hormone Physiology Lab, University of Leuven, Leuven 3001, Belgium
2 Department of Biosystems, Division of Crop Biotechnics, Tropical Crop Improvement Laboratory, University of Leuven, Leuven 3001, Belgium
3 Bioversity International, Leuven, 3001, Belgium

*Author for communication: bram.vandepoel@kuleuven.be
†Senior author.

Abstract

Plant and plant organ movements are the result of a complex integration of endogenous growth and developmental responses, partially controlled by the circadian clock, and external environmental cues. Monitoring of plant motion is typically done by image-based phenotyping techniques with the aid of computer vision algorithms. Here we present a method to measure leaf movements using a digital inertial measurement unit (IMU) sensor. The lightweight sensor is easily attachable to a leaf or plant organ and records angular traits in real-time for two dimensions (pitch and roll) with high resolution (measured sensor oscillations of $0.36 \pm 0.53°$ for pitch and $0.50 \pm 0.65°$ for roll). We were able to record simple movements such as petiole bending, as well as complex lamina motions, in several crops, ranging from tomato to banana. We also assessed growth responses in terms of lettuce rosette expansion and maize seedling stem movements. The IMU sensors are capable of detecting small changes of nutations (i.e. bending movements) in leaves of different ages and in different plant species. In addition, the sensor system can also monitor stress-induced leaf movements. We observed that unfavorable environmental conditions evoke certain leaf movements, such as drastic epinastic responses, as well as subtle fading of the amplitude of nutations. In summary, the presented digital sensor system enables continuous detection of a variety of leaf motions with high precision, and is a low-cost tool in the field of plant phenotyping, with potential applications in early stress detection.

Introduction

It has long been established that plants are not the static organisms they seem at first. Plants can adjust their posture or reorient organs in response to specific developmental and/or environmental signals. Touch-me-not (*Mimosa pudica*) and Venus flytrap (*Dionaea muscipula*) are two well-known species using rapid movements to protect themselves or feed on insects, respectively. In most cases, plants show rather slow movements that are often integrated into growth and development. There are two types of plant movements: nastic and tropic movements (Sisodia and Bhatla, 2018). Nastic movements are triggered by an endogenous or environmental stimulus without a clear directional relationship between the movement and its

Open Access

stimulus, while tropic movements are directional in response to an external (environmental) signal or force.

An example of a nastic movement that is well-integrated in plant development and growth is nyctinasty (or sleep movement), the rhythmic, and diurnal motion of plant organs coordinated by the circadian clock (reviewed in McClung, 2006). These movements are often achieved through bending of plant organs, also known as nutation, caused by differential growth of specific tissues or by the action of motor cells in pulvini. For example, the daily spiral movements (circumnutation) of leaves, flowers, or other organs are dynamic morphological growth outputs of the circadian clock (Apelt et al., 2017).

Besides periodic oscillations, nastic movements can also be induced by external signals. These movements allow plants to cope with adverse conditions and respond adequately to changes in their environment, either to avoid or tolerate periods of stress. One of the best-known examples of this strategy is the low-oxygen escape syndrome, resulting in the hyponastic movement and elongation of petioles to restore the internal oxygen balance (Bailey-Serres and Voesenek, 2008). In Arabidopsis (Arabidopsis thaliana), hypoxic conditions enhance ethylene production, which regulates differential cell expansion in the abaxial and adaxial petiole regions, leading to upward bending of leaves (Polko et al., 2012; Rauf et al., 2013). This hyponastic response has also been observed in Arabidopsis during low light (photonasty; Pantazopoulou et al., 2017) and increased temperature conditions (thermonasty; Park et al., 2019; van Zanten et al., 2012) to avoid shading or radiant heat, respectively. While this upward movement strongly resembles the oxygen escape response, the underlying mechanism is mainly governed by changes in auxin biosynthesis and transport (Pantazopoulou et al., 2017; Park et al., 2019). The opposite response, when leaves bend downward, is called epinasty and has been observed during low-oxygen stress conditions in tomato (Solanum lycopersicum; Jackson and Campbell, 1976). Similarly, bean (Phaseolus vulgaris) leaves show an epinasty-like phenotype during drought stress, to reduce the interception of light and consequently prevent photodamage and wilting (Pastenes et al., 2005).

External signals can also evoke directional movements or tropisms away from or toward the source of these signals. This type of movement enables optimal plant orientation to either facilitate normal development or alleviate stress conditions. Developmentally relevant tropisms include responses such as gravitropism and phototropism. A well-known example of phototropism is the solar tracking movement of leaves (Koller and Ritterl, 1996) or flowers in the direction of the sun, also called heliotropism (Vandenbrink et al., 2014).

Our knowledge about these diverse movements has greatly benefited from advances in phenotyping methods. Standard techniques to assess plant morphology and movements include analog measurements using protractors (Sarlikioti et al., 2011) or indirect methods inferring angular traits from traces (Kazemi and Kefford, 1974; Jackson and Campbell, 1975) or from vertical and horizontal displacements (Jackson and Campbell, 1975; Thomas and Turner, 2001). These methods are quite labor intensive and often lack sufficient resolution, both in terms of space and time. The advent of image analysis has drastically enhanced the sensitivity and quality of motion tracking. For example, advances in computer vision algorithms (Bours et al., 2012; Greenham et al., 2015) have greatly improved our insights in nutational responses.

Image-based phenotyping has become a field of its own, focusing not only on the technology (e.g. LemnaTec, 2021; Phenospex, 2021; WIWAM, 2019) but also on data analysis (e.g. PlantCV (Fahlgren et al., 2015; Gehan et al., 2017), TRIP (Greenham et al., 2015), and OSCILLATOR (Bours et al., 2012)). Camera systems can be integrated into fixed setups to monitor growth or development of small plants such as Arabidopsis (Smeets et al., 2006; van Zanten et al., 2012), or attached to moving platforms to image multiple plants or entire field plots. In field conditions, these platforms are mostly phenotowers (Naito et al., 2017), tractors (Barmeier and Schmidhalter, 2017), or exceptionally field scanning devices (e.g. Fieldscan from Phenospex) or aerial platforms (Wang et al., 2019; Stevens et al., 2020). The output of camera systems can be used to estimate growth and motion-related traits (Binder et al., 2006; Müller and Jiménez-Gómez, 2016; Nagano et al., 2019). However, plant movements and camera orientation are not always optimally aligned. To overcome the phenotyping limitation of orientation and occlusion by other objects and keep track of the movements of individual plant parts, camera systems can be adapted by either moving the camera or the plant during the imaging sequence (e.g. conveyer belt and rotating platform). However, moving or rotating plants can interfere with plant growth and naturally occurring movements (e.g. thigmonasty and thigmomorphogenesis). Alternatively, the spatial configuration of multiple cameras can be optimized to fully capture architectural traits of plants (Shi et al., 2019). In addition, laser scanning or Light Detection and Ranging (LiDAR) has recently gained more attention and allows the accurate measurement of entire plant and canopy geometries. This high-resolution technique has been used to determine geometries and movements in several plant species, such as Arabidopsis (Dornbusch et al., 2014), maize (Zea mays) (Su et al., 2018), birch (Betula pendula) (Wieser et al., 2016), sequoia (Sequoia sempervirens) (Disney et al., 2020), and tomato (Hosoi et al., 2011).

Despite significant advances in imaging technologies, issues with suboptimal orientation, limited spatial resolution, and advanced post-processing algorithms could hamper detailed measurements of certain traits or specific plant organ movements. In this article, we present an easy-to-use digital sensor system as an alternative for analog and imaging techniques, to gather high resolution and real-time data of angular morphological traits. This sensor system allows for the monitoring of both developmental and stimulus-induced dynamic plant movements at a high spatial and temporal resolution. The relatively small sensor modules can be attached to individual plant organs, such as leaves and

stems. This facilitates measuring complex and multi-dimensional processes such as nyctinasty. To further determine its application potential, the sensor system was used to infer species- and genotype-specific movements as well as age-related leaf angle changes. Given the clear impact of abiotic stress on plant morphology, we subsequently monitored (early-)stress effects on leaf angle dynamics of multiple crop species grown under a selection of adverse environmental conditions. We hereby focused primarily on crop species that have large leaves and are known for their morphological flexibility in terms of leaf movements in optimal and suboptimal growing conditions. Finally, we show that the sensors can be used to detect additional growth-related motions such as the concentric expansion of rosette leaves and seedling growth movements. We demonstrate that this digital sensor adds an instrument to the plant phenotyping toolbox that can help advance the field of motion study in plants.

Results

Design of the leaf angle sensor system

The sensor system (Figure 1, A–C) consists of three major components that separate data acquisition and data transfer in time. The first component is a data concentrator (1), that polls data from sensor nodes (2), which are connected to one or more digital sensors (3) capable of measuring angular traits and organ displacement. Both (1) and (2) were designed using Arduino-based microcontrollers and extended with additional communication (Dragino Lora Shield version 1.4) and sensor shields. The Arduino Uno-based configuration of (2) is depicted in Figure 1B. The sensors (3) used in this study were MPU6050 (InvenSense Inc., 2016) sensors, weighing only 5–20 g depending on the cable length used. These inertial measurement unit (IMU) sensors (Figure 1C) are capable of measuring their orientation in two main directions (pitch θ and roll ϕ) and a third minor direction (yaw ψ), which is less consistent and more prone to drift due to its orientation parallel to the field of gravity. The three different movements (pitch, roll, and yaw) are schematically visualized for a compound tomato leaf relative to the fixed plant system in Figure 1D. The leaf can rotate or move with respect to its initial position by bending up or downwards (pitch θ), by rotating around the petiole-leaf tip axis (roll ϕ), or by bearing or rotating in the plane of the leaf (yaw ψ). The stronger the leaf movement, the larger the angle with the vertical axis becomes. Besides these three leaf rotations, the orientation of individual leaflets can also
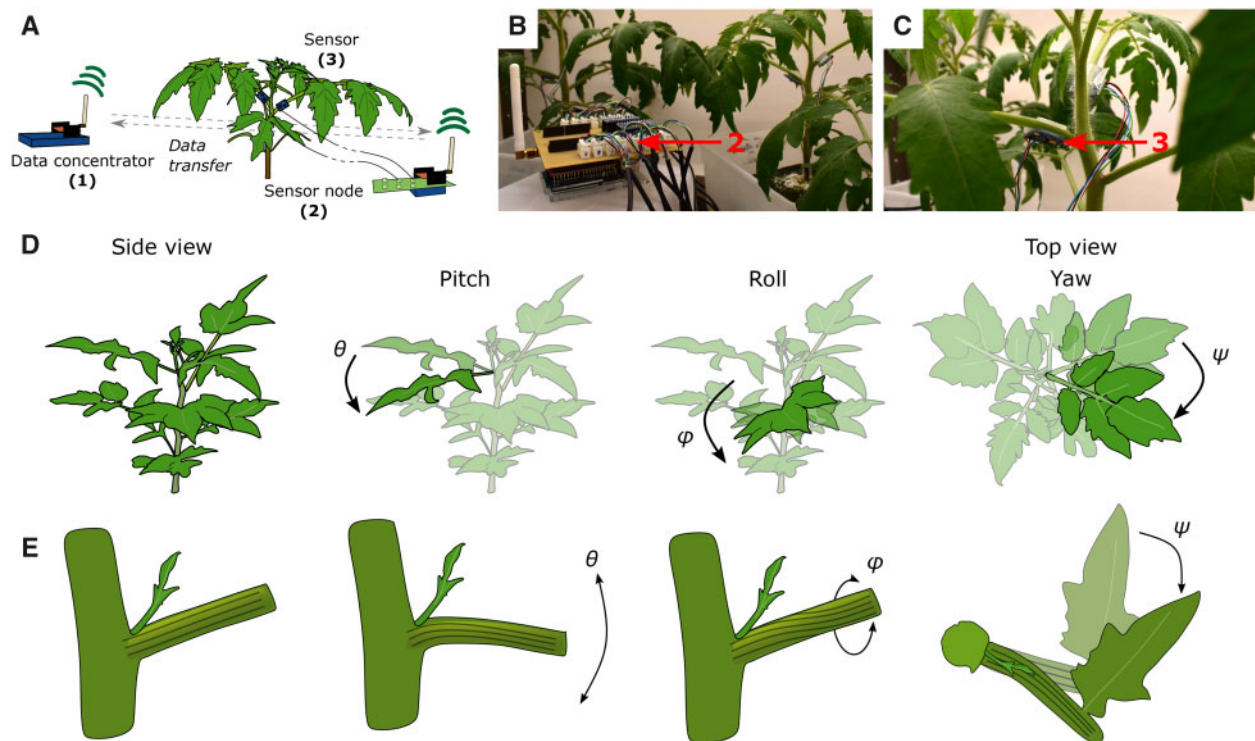
Figure 1 Schematic overview of the components of the sensor system and the different leaf movements. A, The data concentrator (1) sends a data request to sensor nodes (2) that read out data from individual sensors (3) attached to leaves or petioles (tomato example). B and C, Sensor system consisting of a sensor node (2) (Arduino Uno controller, sx1276 Dragino LoRa shield (868 MHZ), and port expander) and IMU sensors (3). D, Schematic representation of leaf movements resulting from rotations around yxz axes. The pitch is defined as the rotation around the petiole–stem boundary axis (up or down) (θ), the roll is defined as the rotation around the leaf rachis axis (ϕ), and the yaw is defined as the rotation around the stem axis (top view) (ψ). E, Close-up representation of the simplified morphological changes in the petiole, resulting in pitch (θ), roll (ϕ), and yaw (ψ) movements depicted in (D).

change, resulting in a more complex leaf movement. The residual leaf posture is the result of morphological changes in organs such as the petiole, and is caused by distortions of the tissue (Figure 1E).

The IMU sensors are connected to sensor nodes through a digital expander or I2C expander shield. The MPU6050 IMU sensor is a microelectromechanical system containing a tri-axis gyroscope and a tri-axis accelerometer. These determine the angular rate and the linear acceleration of the unit, and rely on changes in the internal spring configuration by changes in the Coriolis force or by linear displacement, respectively. Whenever the sensor is rotated, configurational changes evoke changes in sensor capacitances, which are converted to electrical signals. By integrating the internal gyroscope and accelerometer measurements of the IMU in three directions with a digital motion processing (DMP; InvenSense Inc., 2016) algorithm, the angular orientation can be precisely calculated. The orientation, or so-called attitude of the sensors, is expressed following the Tait–Bryan angle convention, in which the body frame, or in this case the leaf frame, is tilted with respect to three main axes. The total tilt is represented as the result of a sequence of intrinsic rotations around the local leaf frame (yaw–pitch–roll sequence).

Prior to deployment in actual experiments, all sensors were calibrated using a standardized calibration system. Due to the nature of the experiments, we focused primarily on pitch and roll movements, and the calibration was done for 64 sensors for the up- and downward movements in one direction (pitch) (Supplemental Figure S1). The variability of the sensor calibration, expressed as the root-mean-square error (RMSE) between measured and actual angles was $5.44°$ when accounting for all sensors ($4.90°$ on a single linear model). The average sensor-specific linear model parameters were: intercept $= -2.07 \pm 5.64°$, slope $= 1.04 \pm 0.05$ (adjusted $R^2 = 0.998 \pm 0.007$, RMSE $= 2.32 \pm 1.91°$). The IMU sensors provide a stable output along a broad range of angular displacements, although the responses toward the maximal angle of $90°$ with respect to the horizontal plane (up and down) become sensitive to gimbal lock and no longer behave linear (Supplemental Figure S1). However, these extrema are often not relevant for measurements of physiological angle dynamics of plants. Sensor stability was assessed for 25 sensors in steady-state conditions (not attached to plant tissue). The sensors were stable for at least 1 week, showing an average drift of $0.026 \pm 0.60°$ and $0.074 \pm 0.51°$ for pitch and roll, respectively, which is negligible compared to on-planta angle dynamics ($8.74 \pm 7.37°$ for pitch and $-1.97 \pm 7.35°$ for roll; Supplemental Figure S2, A–B). The oscillating behavior in steady-state conditions (Supplemental Figure S2, C–D) can be attributed to temperature changes in the sensor environment, and the angular amplitude is small (average daily steady-state amplitude pitch $= 0.36 \pm 0.53°$; roll $= 0.50 \pm 0.65°$; yaw $= 3.44 \pm 4.05°$), especially compared to that of leaf nutations (banana leaf in Supplemental Figure S2). It must be noted that the yaw movement displayed

relatively large oscillations (Supplemental Figure S2, C and D), which could be explained by the orientation of the movement relative to the field of gravity or by the absence of strong yaw movements of the tested banana leaves. Long-term sensor stability was assessed for 12 sensors over a time course of 34 d (Supplemental Figure S3). While intermittent and large angle changes could be ascribed to handling of sensors in between measuring sequences, the within-experiment drift was negligible (Supplemental Figure S3B).

To validate the reliability of the IMU sensor output on planta, the petiole pitch of tomato leaves was compared to petiole angles derived from image analysis using a camera system (Supplemental Figure S4). Image-based and sensor data were strongly correlated (mean $R^2_{adj} = 0.987 \pm 0.007$ and mean RMSE $= 3.92 \pm 4.38°$), indicating that both methods yield similar results in these conditions. In addition, the presence of the leaf angle sensor did not seem to affect the regular pitch movement in the tomato leaves, suggesting that the effect of the sensor weight on the leaf movement was negligible in this case.

Communication between the data concentrator (1) and a sensor node (2) proceeds through Long Range (LoRa) data transfer, enabling the integration of their output in Internet of Things applications. LoRa supports data transfer over several hundreds of meters and even kilometers, restricted by obstructions between the transmitter and the receiver. Depending on the available network infrastructure, data from the sensor nodes can also be gathered through LoRa Wide Area Network (LoRaWAN) gateways connected to a network server. For the data presented in this article, the sensor system was arranged in a local LoRa network. The data concentrator sequentially requests data from individual sensor nodes. These sensor nodes in turn sequentially read-out data from one or multiple sensors (3) and send back the corresponding data vectors. Individual nodes can be distributed over large greenhouse compartments and can theoretically also be deployed in field conditions. The current sensor system relies on AC power supply, but can be adapted to serve in low-power applications driven by batteries or solar energy. To prevent oxidation by high relative humidity (RH) in the greenhouse and occasional splattering from the irrigation system, sensors were treated with a protective coating (Tropicoat).

2D leaf movement monitoring using the angle sensor system

To determine the potential of this sensor system to measure leaf movements in multiple directions, leaf rhythms of tomato and banana plants were monitored over time. Both species have been shown to exhibit a certain degree of leaf motion in at least one principal direction. For tomato (*S. lycopersicum* cv Ailsa Craig), sensors were attached to the petiole base of the leaves to determine the nyctinastic pitch nutations of the leaf (Figure 2A). A clear circadian pattern was observed, in which tomato leaves bend downward with $5-6°$ during the day, and rise up again during the night
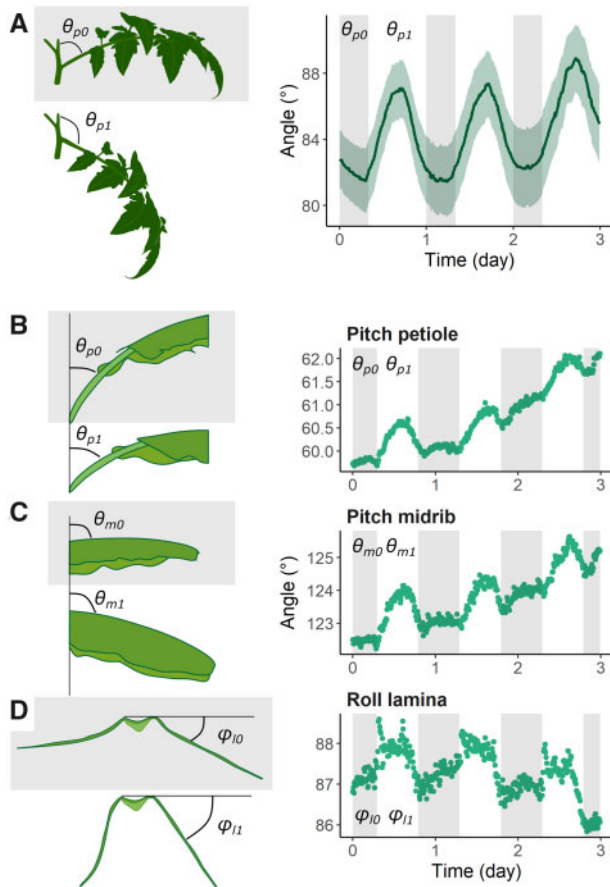
Figure 2 Circadian movements in tomato and banana leaves. A, Diurnal circadian leaf movement profile in the pitch direction of a tomato (cv Ailsa Craig) leaf, together with the 90% confidence interval ($n = 10$). The angle (θ_p) between the main stem and adaxial side of the leaf increased during the day ($\theta_{p1} > \theta_{p0}$) as the leaf curved downward. B–D, Three-day movement of a single banana leaf of *M. acuminata* ssp. *banksii* in the pitch direction represents bending of (B) the petiole (θ_p) and (C) the midrib (θ_m) and (D) the movement in the roll direction represents lamina folding (ϕ_l). Shaded areas represent the dark period (12 PM to 8 AM for tomato, 7 PM to 7 AM for banana). Note the scale difference of the *y*-axis.

(Figure 2A). To assess more complex leaf angle dynamics, we deployed the sensors on different parts of banana (*Musa acuminata* ssp. *banksii*) leaves, as we expected the entire leaf to move (pitch petiole and midrib) and the leaf laminae to fold (roll leaf laminae) (Figure 2, B–D). The large leaf size of banana facilitates attaching multiple sensors to the same leaf. To monitor this complex leaf movement, sensors were attached to the petiole base, the central point of the midrib, and the center of the left leaf lamina (Figure 2, B–D). Banana leaves also showed a clear rhythmicity in their pitch movement of the petiole and, subsequently, of the entire leaf. The nutations of these leaves had a more distinct day–night cycle, characterized by a relatively stable orientation at night (night θ_0 and day θ_1 in Figure 2, B–D). In addition, banana leaves showed a lamina roll movement

of ~1–1.5°, demonstrating the sensitivity and robustness of the sensor system.

Circadian leaf movements are determined by age and genotype

Our initial leaf angle measurements showed that the sensor system is able to capture circadian rhythms of both tomato and banana leaves. We subsequently measured this trait for middle-aged and younger leaves (Leaves 4–6; Figure 3A) of tomato plants in the seventh and eighth leaf stage. In this developmental stage, Leaf 4 is almost fully grown, while Leaf 5, and especially Leaf 6 are still expanding. The ontogenetic differentiation of the leaf oscillations was assessed for three morphologically different tomato accessions (Figure 3B). A physiological age difference of approximately one leaf in the Ailsa Craig cultivar resulted in distinct leaf movements (Figure 3A). Young leaves of younger plants bend down at a higher rate and seem to have a more distinct daily leaf nyctinasty, which gradually fades as leaves or plants age (Figure 3A). The corresponding daily amplitudes of the different leaves and plant ages are depicted in Supplemental Figure S5. The circadian movements are, however, highly genotype-specific. The Russian parthenocarpic cultivar Severianin lacks the distinctive daily rhythm observed in Ailsa Craig or Cuba Plum, a Cuban variety. The latter is characterized by an even larger angular amplitude of the young leaves (Supplemental Figure S5). In addition, older leaves of Severianin are more horizontally oriented, as demonstrated by the larger overall leaf angle. In general, leaves of the three tomato cultivars gradually move down over time (6 d; Figure 3B).

Both leaf orientation and daily nutations are also highly dependent on the genetic background in banana. We compared the three different leaf movements (petiole pitch, midrib pitch, and lamina roll) of three different banana genotypes (*Musa balbisiana*, *M. acuminata* ssp. *banksii*, and *M. acuminata* ssp. *malaccensis*; Figure 3C). The data presented in Figure 3C were centered to the starting angle of the individual leaf to better compare circadian rhythms. The corresponding raw angle data are provided in Supplemental Figure S6. In terms of leaf orientation, *M. balbisiana* had more upright petioles (lower pitch at the petiole base) and open leaf laminae (lower roll of the laminae) as compared to *M. acuminata* ssp. *malaccensis* and *M. acuminata* ssp. *banksii* (Supplemental Figure S6). Interestingly, *M. balbisiana* seemed to respond stronger to the day–night transition than the other genotypes, resulting in more pronounced amplitudinal changes within the same day (Figure 3C). The leaf movement of the two *M. acuminata* subspecies was very similar, although leaf curling at the midrib proceeded more rapidly in *M. acuminata* ssp. *banksii* over the 3-d period.

## Abiotic stress drastically alters the diurnal leaf movements in tomato and banana

Abiotic stress responses oftentimes involve major leaf movements such as epinasty or hyponasty. One of the most
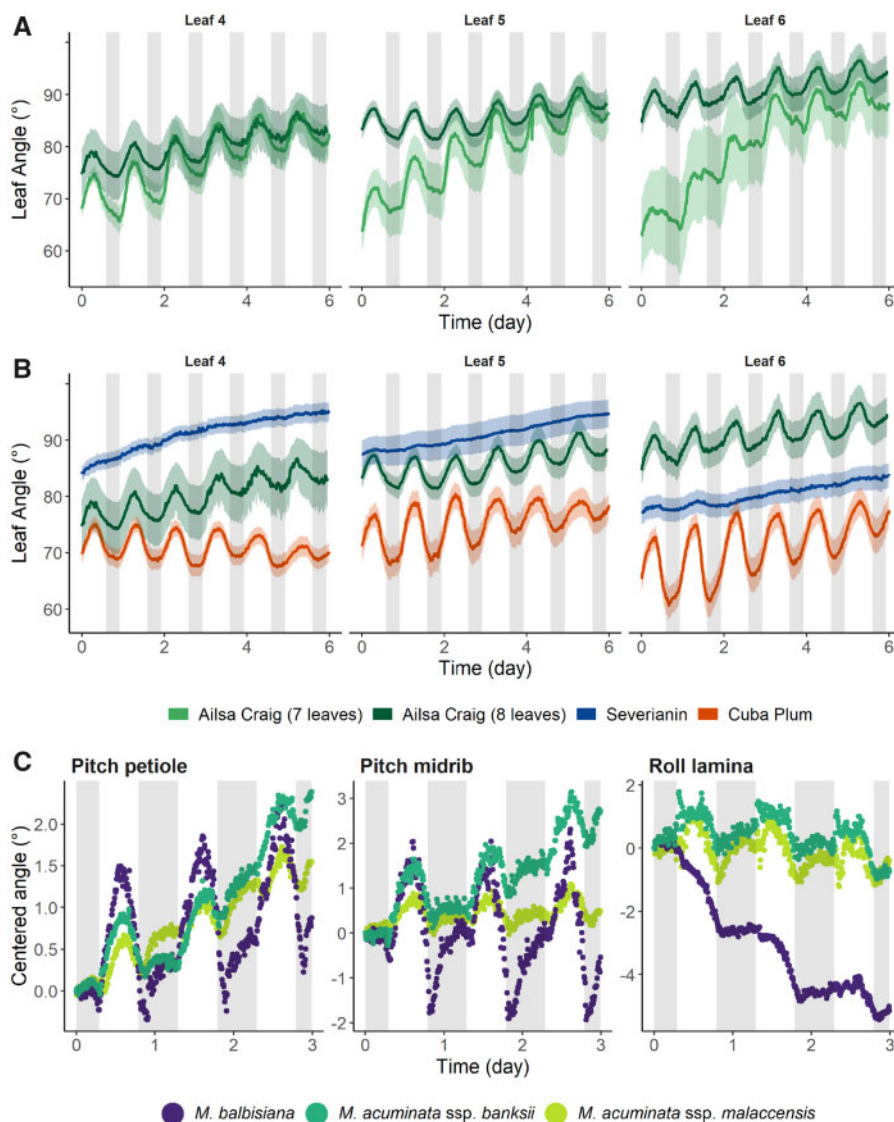
Figure 3 Age- and genotype-specific circadian leaf movements in tomato and banana. Circadian rhythms of leaf pitch movements (θ_p) of (A) leaves of different ages of tomato plants (cv Ailsa Craig) at a different plant age (7 and 8 leaves on average) ($n = 10$) and (B) of leaves of different ages in three distinct tomato accessions (cv Ailsa Craig, Severianin and Cuba Plum) ($n = 10$). Leaf 4 was the oldest true leaf, followed by leaves 5 and 6. Shaded polygons represent the 90% confidence interval. C, Circadian rhythms of the pitch movement of the leaf petiole (θ_p) and midrib (θ_m) and the roll movement of the leaf lamina (ϕ_l) of single leaves of three banana genotypes (Leaf 3 *M. balbisiana*, Leaf 4 *M. acuminata* ssp. *banksii*, and Leaf 2 *M. acuminata* ssp. *malaccensis*). Data in (C) were centered to the starting angle. Lines in (A and B) represent average leaf angles $\pm$ the confidence interval. Shaded areas represent the dark period (12 PM to 8 AM for tomato (A and B), 7 PM to 7 AM for banana (C)).

striking epinastic responses can be found in tomato during waterlogging. We used our sensor system to measure the magnitude and dynamics of the epinastic curvature of tomato leaves during a 3-d waterlogging treatment and monitored the subsequent recovery period. High oxygen consumption rates were observed in the root zone of Ailsa Craig plants, leading to root hypoxia (Supplemental Figure S7). Soon after reaching hypoxic conditions, leaves started bending downward (Figure 4A), leading to a remarkable decrease of the canopy cover (Supplemental Figure S8). Young leaves (Leaf 6 in Figure 4A) seemed to recover faster after the hypoxia treatment, and also restored their horizontal position faster once reoxygenation occurred.

Previous reports have also described an epinastic response during high salinity conditions in the root zone (Jones and El-Beltagy, 1989). However, we did not observe a strong epinastic curvature using our sensor system (Figure 4B; Supplemental Figure S9). Interestingly, both salt and drought stress primarily influenced circadian leaf oscillations, that appeared to fade out faster compared to control plants, albeit only mildly (Figure 4, B and C). Although not significant (Supplemental Figure S10), this decline in nyctinasty was more prominent when drought conditions became severe (R1–R2 transition in Figure 4C), and this response seemed to occur predominately in older leaves. Surprisingly, a sudden discontinuation of regular fertigation (R3 in Figure 4C),
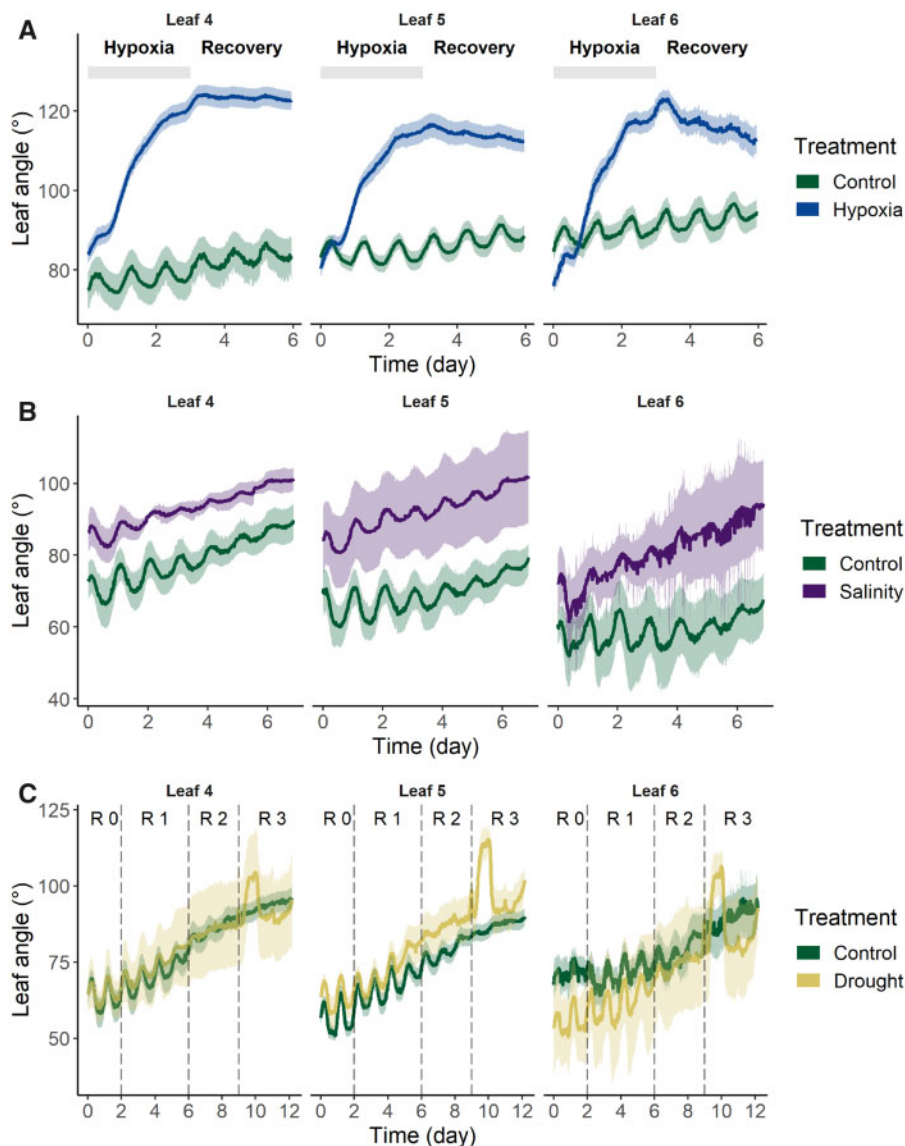
Figure 4 Pitch movements (θ_p) of leaves of different ages (fourth, fifth, and sixth leaves) during different abiotic stress conditions in tomato (cv Ailsa Craig), together with the 90% confidence interval. A, Waterlogging treatment of 3 d (shaded bar) and stress recovery after reoxygenation ($n = 10$); (B) salt treatment with sodium chloride enriched fertigation for 7 d (EC = 10; $n = 4$); C, drought treatment with decreasing watering regimes: R0 = well-watered; R1 = irrigation in the morning and the evening; R2 = irrigation only in the morning; R3 = no irrigation ($n = 4$–8).

triggered a peak in leaf angular response (sudden drastic downward leaf movement followed by a fast recovery) for leaves of all ages. This observation suggests that there is some hydrological entrainment for periodic irrigations, and that a sudden total deprivation of irrigation leads to an abrupt but temporary leaf movement that lasts about 24 h, after which the leaves seem to partly recover toward a more horizontal petiole angle. At the end of the drought experiment, plants started to show wilting symptoms and as a result, the leaf angle increased again (transpiration data in Supplemental Figure S11).

We wondered if these drought-induced changes in leaf movements can also be detected in other plant species. Therefore, we performed a drought experiment on three banana genotypes originating from regions with different

environmental conditions and assessed their canopy cover changes and leaf movements (see illustration Figure 5A). We observed a genotype-specific canopy cover response to drought stress, with *M. balbisiana* being less prone to drought-induced canopy cover changes (Figure 5B). Although this trait might be useful to describe the overall canopy behavior during water deficit, it is too coarse to entirely capture complex leaf movements. Our measurements of leaf and lamina orientation showed a different responsiveness between genotypes during the drought treatment (Figure 5C; noncentered data in Supplemental Figure S12). Both *M. balbisiana* and *M. acuminata* ssp. *malaccensis* showed a moderate change in daily leaf movement (2–2.3° for the petiole base and 4.7–6.9° for the petiole midrib), while *M. acuminata* ssp. *banksii* showed a more pronounced
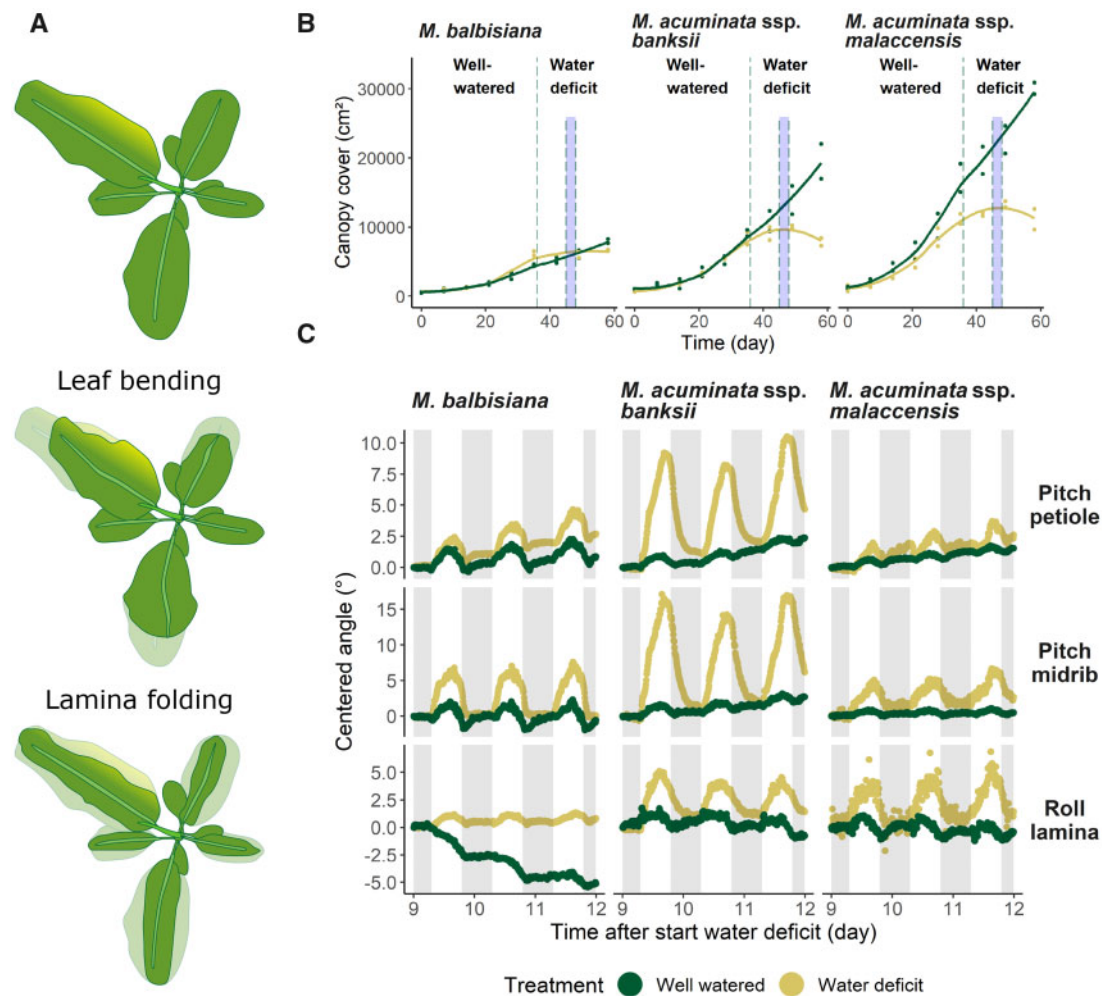
Figure 5 Circadian leaf movements of banana during drought stress. A, Illustration of different canopy cover changes in banana as a result of complex leaf movements in multiple directions. B, Canopy cover change of the three banana genotypes (*M. balbisiana*, *M. acuminata* ssp. b*anksii*, and *M. acuminata* ssp. *malaccensis*) throughout the entire drought experiment for both well-watered (green) and water deficit (yellow) conditions. The dashed line in (B) indicates the end of irrigation and the shaded region between dashed lines corresponds to the 3-d period of leaf angle measurements of (C). C, Comparison of single leaf movements measured at the petiole (θ_p), midrib (θ_m), and lamina (ϕ_l) for three banana genotypes in well-watered (green) and water deficit (yellow) conditions. Data in (C) were centered to the starting angle. Shaded areas in (C) represent the dark period (7 PM to 7 AM).

downward leaf bending (8° at the base and 15° at the midrib) during drought stress. The roll movement of the leaf laminae was more prominent in *M. acuminata* ssp. *banksii and M. acuminata* ssp. *malaccensis*, showing that there is a stronger inward lamina folding in these genotypes. The progression of the water deficit and its effect on the hourly transpiration is provided in Supplemental Figure S13. While total cumulative transpiration is higher in the *M. acuminata* genotypes in well-watered conditions, water deficit results in a similar cumulative water loss of the three genotypes at the time of leaf angle measurements.

Species-specific leaf movements during waterlogging
The epinastic leaf movement, as shown for tomato in Figure 4A, is a characteristic response to waterlogging (Jackson and Campbell, 1976). We wondered whether these hypoxic stress conditions also influence leaf movements in

other species with varying degrees of morphological similarity or different motoric mechanisms. Leaf movements, or the absence thereof, might relate to the performance of these species under low-oxygen stress. Therefore, we monitored the waterlogging response of several leaves of two Solanaceae species (potato and bell pepper) and two other species (cucumber and bean) using the leaf angle sensor system (Figure 6). The corresponding concentrations of dissolved oxygen in the plant containers are depicted in Supplemental Figure S7. For potato, oxygen deprivation of the root system triggered a strong epinastic response, similar to the one observed in tomato, although the magnitude of the angle change for both the initial response and the recovery seemed to be less pronounced (Figure 6A; Supplemental Figure S14). This characteristic downward leaf movement was not observed for bell pepper, cucumber and bean. Nevertheless, we were able to visualize other species-specific
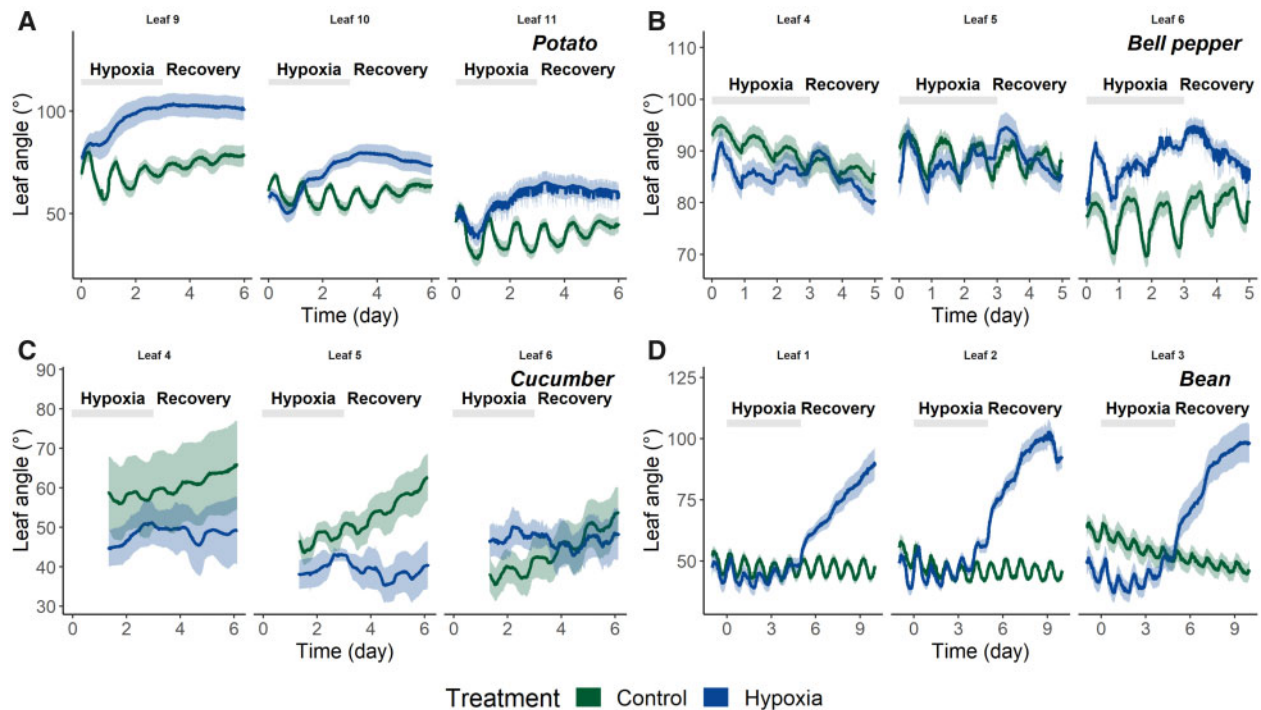
Figure 6 Leaf movements during waterlogging stress for different species. A, The epinastic response of the pitch movement (θ_p) of three potato leaves (9th, 10th, and 11th leaves) during and after 3 d of waterlogging ($n = 9$). B, The effect of a 3-d waterlogging treatment on three bell pepper leaves (fourth, fifth, and sixth leaves) showing an altered circadian rhythm ($n = 10$). C, Cucumber leaves (fourth, fifth, and sixth leaves) also show a reduced circadian rhythm after a 2-d waterlogging treatment ($n = 5$). D, Bean leaves (first, second, and third leaves) show a strong downward bending predominately during reoxygenation ($n = 10$). Shaded polygons represent the 90% confidence interval and shaded bars represent the waterlogging period.

leaf movements during and after a period of waterlogging. Bell pepper leaves showed a short peak response, after which they returned to their initial orientation and continued their circadian oscillations, albeit at a smaller amplitude (Figure 6B; Supplemental Figure S15B). One day after reoxygenation, the bell pepper leaves showed a gradual upward movement (hyponasty). For cucumber, the effect of the hypoxia treatment was mostly confined to a decrease in the amplitude and a seemingly shifted period of the circadian rhythm of the leaf oscillations, especially after reoxygenation (Figure 6C; Supplemental Figure S15C). Common bean plants were characterized by a stable and consistent nutational rhythm during waterlogging (Figure 6D). The amplitude of the corresponding oscillations slightly decreased in the older leaves, although not significantly (Supplemental Figure S15D). Despite the waterlogging treatment, the oxygen concentration in the root zone did not reach the same hypoxic levels as observed for tomato, potato, and bell pepper (Supplemental Figure S7). Nevertheless, leaves showed mild epinasty toward the end of the treatment, and a remarkably strong downward bending during reoxygenation, corresponding to wilting.

Growth monitoring using angular dynamics

Besides monitoring leaf orientation, the sensor system could also capture growth dynamics, as can be observed in the steady downward movement in growing tomato leaves in Figures 3 and 4. To illustrate the growth-related movements in species with a different architecture and development, we focused on the outward rosette expansion of lettuce (*Lactuca sativa*) and seedling growth of maize (*Z. mays*), which is characterized by radial leaf emergence. For lettuce, we measured the orientation of two easily accessible leaves on opposite sides of the rosette for three lettuce cultivars (Lugano, Fairly, and Lucrecia), and observed a gradual downward movement of the leaves over time. This movement was probably related to the expansion of the lettuce rosette, pushing the outer leaves further down, thus corresponding to growth of the lettuce head (Figure 7, A and B). Daily nutations seemed to fade out during rosette growth, and leaves moved toward a steady-state position, suggesting that there is a degree of lettuce head compactness. The species-specific rosette growth was validated by assessing the canopy cover (Figure 7C). Depending on their size and position, flattening of the outer rosette leaves might result in actual canopy cover changes. Lugano showed less leaf movement, probably due to its more compact and curly rosette shape.

Seedling growth of maize plants was assessed by attaching an IMU sensor vertically to the stem. At first sight, growing maize seedlings move in a seemingly irregular and erratic fashion (Figure 8A), especially in comparison to the nyctinastic nutations of tomato or banana leaves (Figure 2). Although the daily rhythmic oscillations in maize stems are largely absent, day–night transitions still seem to govern
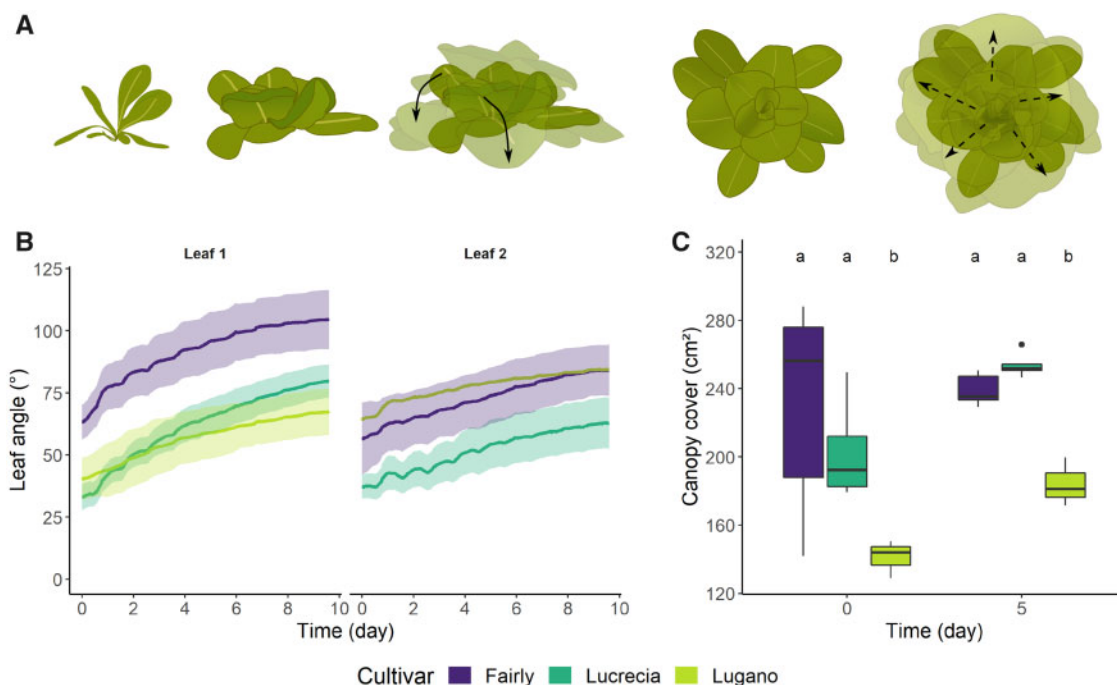
Figure 7 Leaf movements in the rosette of three lettuce cultivars. A, Leaf and canopy changes during lettuce rosette growth. Old leaves are pushed down by the compact and concentric growing lettuce head. B, Pitch orientation (θ) of two leaves on the opposite sides of the lettuce head of three different cultivars, together with the 90% confidence interval ($n_1 = 6$; $n_2 = 6$; $n_3 = 4$ and 3 for leaves 1 and 2, respectively). C, Boxplot representation of the canopy cover changes derived from leaf projections in top view images for the three cultivars after 5 d of growth (center line = median, box limits = first and third quartile, whiskers = largest and smallest value within 1.5 × interquartile range).
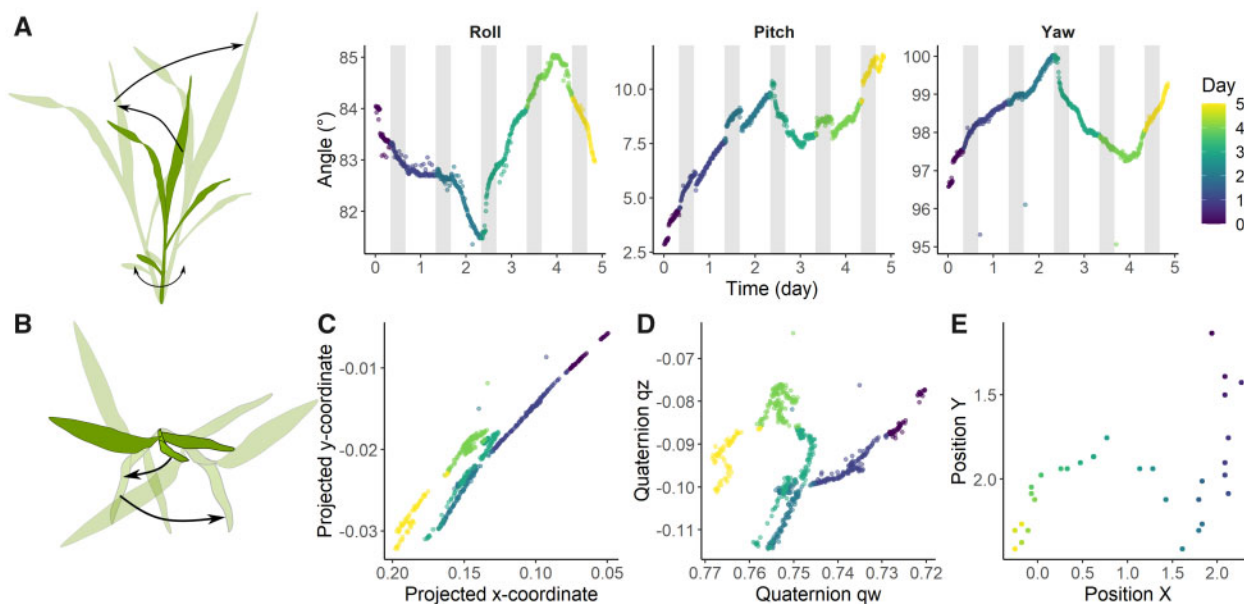
Figure 8 Motion in a single growing maize seedling, derived from sensor measurements at the stem base. A, Side view of a maize seedling, together with the angle representation of the stem during its growth (yaw ψ, pitch θ, and roll ϕ). B–E, "Top view" comparison between (C) horizontal projection of the unit vector trigonometrically derived from the orientation in (A), (D) quaternion representation and (E) actual sensor position based on top-view image analysis (see Supplemental Figure S16). The x-axis in (C and D) and y-axis in (E) were reverted to facilitate comparisons between representations.

some directionality of the seedling movement. To better understand and visualize this complex growth motion, angular data from the sensor were projected as unit vectors to the horizontal plane (Figure 8C; see "Materials and methods") and subsequently also converted into quaternions (Figure 8D), a vector-based representation using complex

numbers to define angular movement and the orientation of an object. To validate this result, we compared the sensor-derived trigonometric projection and quaternion data with horizontal projections derived from top view images (Figure 8E; image examples in Supplemental Figure S16). Although rudimentary, the conversion of angular data into trigonometric projections or quaternions reveals a certain level of similarity with real tropic motions in growing maize seedlings. The segmented nature of this motion indicates that seedling movements can be gradual throughout the day, but might shift between days. Differences between the above representations could partly be ascribed to suboptimal tracking of the images and to the sensor orientation relative to the camera.

Discussion

Digital sensors for continuous monitoring of plant motions

While the importance of leaf inclination angle for crop breeding and plant growth has been widely acknowledged (Sarlikioti et al., 2011; Mantilla-Perez and Salas Fernandez, 2017; Itakura and Hosoi, 2019; Dou et al., 2020), many recent image and scanning-based techniques mainly focus on growth-related traits (Fahlgren et al., 2015). Stereo-vision methods have been successfully applied to determine leaf-angle distributions of canopies of for example sugar beet (*Beta vulgaris* ssp. *vulgaris*), barley (*Hordeum vulgare*; Müller et al., 2015; Müller-Linow et al., 2015), and soybean (*Glycine max*; Biskup et al., 2007). However, these studies also recognize the limitations of reliable leaf angle estimates at certain, mostly steeper, leaf orientations. More sophisticated setups with multi-view camera systems (Paproki et al., 2012; Shi et al., 2019) or laser scanning methods (Golbach et al., 2016; Itakura and Hosoi, 2019; Jin et al., 2019) have yielded detailed 3D information on plant and even organ architecture by implementing advanced matching and segmentation algorithms. Curve and plane fitting through individually segmented petioles or leaves can subsequently be used to determine the petiole angle (Paproki et al., 2012) or the leaf face orientation, respectively (Thapa et al., 2018). Matching of individual petioles in an image sequence requires optimal positioning of the device toward the plant and is sensitive to plant movements between subsequent measurements, possibly occluding the organ of interest (Paproki et al., 2012). We encountered this issue together with growth-induced repositioning of the organ itself during sensor validation, leading to partial data loss and a possible baseline shift (Supplemental Figure S4). Furthermore, obtaining continuous data for a large number of plants requires multiple or moving imaging systems, corresponding to significant hardware costs for large-scale phenotyping experiments.

Our IMU sensor system is able to record dynamic leaf movements in real-time, allowing for continuous monitoring of plant motion without the need of image analysis. Furthermore, attaching the sensor directly to, for example, a petiole, circumvents problems with miss-matching and occlusion. The sensor system is not sensitive to variability in illumination nor does it rely on large-scale imaging booths or conveyor belts as often used for image-based phenotyping. Their low cost facilitates the deployment of multiple sensors to simultaneously monitor leaf movements in a setup with several plants and individual leaves. The sensors can be distributed over a large area such as a greenhouse or potentially even a field, as the system relies on LoRa technology for data transfer. Its efficiency will largely depend on the distance between the transmitter and receiver and on their surroundings. By strategically arranging these communication components or by integrating them in another network topology (e.g. LoRaWAN), data can be gathered from several sites and potentially also combined with other types of data. The accuracy of our sensor system to measure angular traits ($2.32 \pm 1.91°$ for a sensor-specific linear model of the pitch) is comparable to that of other methods using stereo-vision (1.9–5°; Biskup et al., 2007) or laser scanning (2.5°; Itakura and Hosoi, 2019). With an estimated average steady-state oscillation of $0.36 \pm 0.53°$ for the pitch and $0.50 \pm 0.65°$ for the roll movement, IMU sensors can detect subtle variations in leaf orientation. In addition, they are capable of providing information on 2D leaf orientation (combining pitch and roll) in time, irrespective of changes in leaf posture that complicate acquiring image-derived traits.

Despite these clear advantages, the sensor system might not be suitable for certain applications and can benefit from further improvements. For example, young seedlings or small plants such as Arabidopsis, might suffer from the weight of the sensor (5–20 g), leading to biased plant movements. Connecting sensors to certain plant organs could also influence their growth or movements, although we have not observed any damage or large sensor-induced changes in morphology (Supplemental Figure S4). The fact that we were able to reliably measure daily leaf nutations strengthens this observation. In terms of sensor design, miniaturization and modifications supporting harsh or outdoor environments would largely expand the application potential of the system in the field. Currently, it has only been used in controlled conditions such as growth chambers and greenhouses. Under field conditions, the current need for a power supply and the wired design might pose a number of practical limitations. By optimizing the communication protocol and limiting the number of sensors connected to an individual node, the network could more easily be organized as a wireless system. This setup would largely reduce power consumption, resulting in a stand-alone system with integrated batteries, that could be deployed in the field.

Circadian leaf movements are age-, genotype-, and species-dependent

The angle of a tomato leaf changes during development (Sarlikioti et al., 2011), which is a possible strategy to optimize light interception throughout the canopy (Papadopoulos and

Pararajasingham, 1997). The inclination angles derived from our sensor system are in line with those reported in previous studies (Sarlikioti et al., 2011; Chen et al., 2014; Dieleman et al., 2019) and depend on the respective leaf and plant age (70–100°; Figure 3). Age effects on leaf angle distributions have also been observed in other species, such as sugar beet (Müller et al., 2015; Müller-Linow et al., 2015), indicating that leaf reorientation provides a degree of flexibility for light interception at different developmental stages. Another aspect of leaf movements that depends on the developmental stage and that is determined by specific circadian regulatory pathways are daily leaf nutations. This is not surprising, given the fact that the circadian clock itself differs in young and old leaves (Kim et al., 2016), resulting in a shift of the circadian period. As a result, daily leaf nutations, as an output of the circadian clock, are likely subject to a certain degree of developmental control as well. In Arabidopsis, circadian movements have previously been linked to environmental (Bours et al., 2013; Apelt et al., 2017), genetic, and growth aspects (Dornbusch et al., 2014). Many hormones are, to some extent, also controlled in a diurnal fashion (reviewed in Atamian and Harmer, 2016) and might contribute to the regulation of nyctinasty in tomato. For example, ethylene has been shown to regulate elongation (Polko et al., 2012) and is in part responsible for circadian leaf movements through the integration of external signals such as light and temperature (Bours et al., 2013). In fact, ethylene production itself is also determined by the circadian clock (Thain et al., 2004). Gibberellins (GAs) have also been linked with petiole elongation in tomato (Schrager-Lavelle et al., 2019) and Arabidopsis (Tseng et al., 2004). Both GA biosynthesis (Hisamatsu et al., 2005) and signaling (Arana et al., 2011), and subsequently petiole elongation are partly regulated by the circadian clock in Arabidopsis. Besides this circadian regulation, light periodicity and light quality play another key role in the rhythmic and GA-related elongation (Hisamatsu et al., 2005; de Lucas et al., 2008). A disrupted GA metabolism might explain the lack of diurnal leaf movement in the tomato cultivar Severianin (Figure 3B). This accession has a mutation in the *pat-2* gene, which previously has been linked to GA contents in un-pollinated ovaries (Fos et al., 2000). However, its role in regulating petiole movement remains unknown. Genotype-specific differences in leaf oscillations (Figure 3B) have also been linked to the circadian clock (Müller et al., 2015, Müller-Linow et al., 2015). Apparently, variations in cotyledon movements between cultivated and wild tomato accessions can be attributed to domestication, specifically targeting LNK2 and EID1, two mediators of the light-dependent regulation of the circadian clock (Müller et al., 2018).

We observed that there is also a genotypic variability in the daily rhythms of banana leaf movements (Figure 3). Our results indicate that *M. balbisiana* has a stronger oscillatory motion of the petiole than two *M. acuminata* genotypes. Diurnal lamina folding in banana has been proposed as a protective strategy against excess light to prevent

overheating and photo-inhibition (Thomas and Turner, 2001), similar to the paraheliotropic response in beans (Pastenes et al., 2005). Lamina folding seems to occur mainly under strong evaporative demands (Stevens et al., 2020), but composite leaf movements in banana have not yet been described.

Abiotic stress directs certain leaf movements in an age- and species-specific manner

Morphological adaptations are well-known responses of plants to changes in environmental conditions. The reorientation of leaves during stress is one of the most striking and visible adaptations and is, to a large extent, regulated by alterations of the metabolism and transport of hormones. Induction and transport of auxins direct the hyponastic movement of Arabidopsis leaves during suboptimal light (Pantazopoulou et al., 2017) and temperature (Park et al., 2019), while ethylene entrapment evokes a similar response during low oxygen conditions (Polko et al., 2011). In contrast to the hyponastic response observed in Arabidopsis, leaves of certain species such as tomato undergo epinasty during waterlogging (Jackson and Campbell, 1976). Both of these nastic movements have been attributed to an altered ethylene metabolism, either by accumulation of ethylene gas due to diffusion barriers in water (Sasidharan et al., 2017), or by upregulation of its biosynthesis pathway (Bradford and Yang, 1980). Within the *Solanaceae* family, differentiation of epinasty in response to ethylene has been previously observed (Edelman and Jones, 2014), as well as of their plasticity to waterlogging (Hartman et al., 2020). Our results show that there indeed exists a differential responsiveness of species such as tomato, potato, and bell pepper to waterlogging, but also that leaf age plays a substantial role in this epinastic response (Figures 4 and 6). In bell pepper, for example, only younger leaves show strongly altered movements due to the waterlogging treatment, while in tomato these younger leaves are the first to recover after reoxygenation. This age-dependent plasticity, although often overlooked, is undeniably a major mediator of abiotic stress resilience in plants (reviewed in Rankenberg et al., 2021).

Interestingly, our sensor-based system revealed that root hypoxia did not entirely abolish the circadian leaf movements of tomato and potato during the first hours of the treatment (Figures 4 and 6; Supplemental Figure S15), indicating that the regulation of epinasty is gated by the circadian clock. In the past, analog measurements of flooding-induced epinasty in tomato were not able to distinguish this kind of circadian entrainment (Bradford and Yang, 1980; Else and Jackson, 1998). The gating mechanism provides plants with a way to adequately control abiotic stress responses in a circadian fashion (Greenham and McClung, 2015; Grundy et al., 2015). Similarly, the circadian clock also gates the shade-avoidance response leading to petiole elongation in Arabidopsis (Salter et al., 2003; Mullen et al., 2006).

Water deficit induces changes in plant water use and hydraulic conductance (Caldeira et al., 2014), and evokes adaptive responses, such as absciscic acid-mediated feedback to the circadian clock (Marcolino-Gomes et al., 2014; Grundy et al., 2015). The effect of drought on diurnal leaf movements is less studied, except for some reports on the enhanced paraheliotropic response in banana laminae (Thomas and Turner, 2001; Stevens et al., 2020) and leaf rolling in maize (Baret et al., 2018). Both of these movements are, however, important indicators of drought stress, also observed in other monocot species such as wheat (Verma et al., 2020) and rice (Cal et al., 2019) and are determined mainly by leaf morphology (Cal et al., 2019). Our analysis of leaf movements during water-deficit stress in *M. balbisiana*, a drought resilient banana genotype (Van Wesemael et al., 2018), originating from drought-prone regions (Perrier et al., 2011; Kissel et al., 2015; Eyland et al., 2021), showed less lamina folding compared to two *M. acuminata* genotypes, indicating that *M. balbisiana* is less responsive toward dry conditions (Figure 5). Whether or how lamina folding and entire leaf movements are related to this drought response is not yet known, although our results show that petiole bending and leaf curling are both enhanced by drought stress (Figure 5). Each of these individual movements provides a means to regulate the evaporative surface and might contribute to the overall performance of banana leaves and plants. Other drought-induced leaf movements, such as epinasty, reduce interception of light and prevent dehydration in bean (Pastenes et al., 2005; Lizana et al., 2006), apricot (Ruiz-Sánchez et al., 2000), and grapevine (Briglia et al., 2020). Interestingly, leaves of tomato plants exposed to drought stress first seem to dampen their circadian leaf movements at the onset of dehydration, after which they undergo a sudden but reversible downward movement during severe water deficit (Figure 4). This nonrhythmic response could be attributed to temporary wilting due to extreme turgor loss followed by restoration of the turgor pressure. Although there is no clear evidence for this sudden behavior, recovery of turgor pressure without additional water supply has been observed in cabbage leaves (Levitt, 1986) and might be related to solute redistribution (Weisz et al., 1989) or to light-dependent changes in stomatal resistance (Lynn and Carlson, 1990; Ache et al., 2010).

Salinity stress did not evoke drastic changes in leaf movements in tomato, in contradiction to earlier studies (Jones and El-Beltagy, 1989). These authors observed differences in responsiveness between leaves of different ages for different tomato cultivars, but assessed the inclination angle only after a 4-week treatment. Other studies (El-iklil et al., 2000) reported rather moderate changes, that might support our own observations in young leaves (Figure 4; Supplemental Figure S9; difference of mean daily trend change between high salinity and control $\Delta = -0.35°$ for Leaf 4, $\Delta = 1.05°$ for Leaf 5, $\Delta = 2.08°$ for Leaf 6). Similar to the drought response, salinity stress caused a dampening of the circadian oscillations, predominantly in older leaves (Supplemental Figure S10A). Hypothetically, this premature dampening of circadian movements could be ascribed to a stagnation of cell elongation and subsequent growth of the leaf caused by suboptimal conditions such as drought (Caldeira et al., 2014; Clauw et al., 2015; Dubois et al., 2017).

Plant motions are indicative for leaf and plant development

Besides circadian oscillations or movements controlled by the environment, plant motions can also be directed by growth and development, which are often intertwined (Dornbusch et al., 2014; Riviere et al., 2017). Plant growth and leaf aging together determine leaf orientation and inclination. For example, aging beet plants show an increasingly planar shape, which has been linked to the progressively changing light conditions in the field, as well as a light-independent downward leaf movement (Müller-Linow et al., 2015). In the prairie forb *Silphium terebinthinaceum*, the growing rosette pushes down the outer leaves, resulting in a more horizontal orientation of older leaves (Smith and Ullberg, 1989). We observed a similar response in older lettuce leaves during rosette growth (Figure 7). In addition, growth influences leaf weight and tissue elasticity, which typically leads to an enhanced gravitropic response, thus increasing leaf angle, mainly in older leaves (Hernandez, 2010). Leaf angles can also be controlled by more complex developmental cues. For example, in maize, *ZmCLA4* has been identified as a regulator of leaf angle and plant architecture, resulting from its effect on auxin flow and shoot gravitropism (Zhang et al., 2014; Dou et al., 2020). Changes in mechanical properties of petiole cells and the increasing weight of growing leaves have most likely contributed to the age-related differences in leaf angle, as observed in tomato, potato, bell pepper, and cucumber (Figures 3, 4, and 6).

It is not surprising that growth movements are regulated by development and appear early in the plant's life cycle (Riviere et al., 2017). For example, young maize seedlings show short oscillatory bursts of the hypocotyl, which are likely caused by leaf emergence and the subsequent alternations of the energy metabolism and growth rate (Ciszak et al., 2016). Later in their development, maize plants no longer exhibit these frequent bursts, but show larger, more gradual and low-frequent movements (Figure 8). It is very likely to assume that these movements are the result of meticulous and time-specific organization of graviception, autotropism (Hamant and Moulia, 2016), and ultimately posture control (Bastien et al., 2014, 2018; Moulia et al., 2019). Interestingly, our sensor analysis of maize seedling stem orientation suggests that stem motion is related to the outgrowth of leaves into a certain direction, although our time-lapse images indicate that there is a phase difference between mass distribution and actual leaf position. To fully characterize complex motions such as growth movements in maize seedlings, the

relationship between ground truth and sensor orientation could be further explored.

Conclusions

In this article, we show that it is possible to measure the dynamics of complex movements of plants and plant organs in real-time with a digital inertial measurement sensor. Both small-scale changes in leaf orientation, such as nyctinastic nutations and larger, mostly stress-induced movements, such as epinasty can be monitored at a high temporal and spatial resolution. It has become clear that not only the growth conditions, but also leaf and plant age, strongly determine motion responses, in conjunction with the circadian clock. Furthermore, leaf movements are affected by changes in the environment and the resulting leaf dynamics depend on the nature of the abiotic stress. Gradual down or upward bending and dampening of the circadian rhythm are two possible modes of stress-specific changes in leaf attitude. Young leaves seem to be more resilient to the long-term effect of waterlogging on leaf posture, although this is highly species-specific and might not be generalized for other stress conditions.

Digital motion sensors are a suitable alternative to imaging techniques to monitor normal and stress-induced movements of plants, especially when the plants or plant parts are not entirely visible. In this respect, direct sensor contact can reveal valuable insights into complex and dynamic plant motions. The current design of the MPU6050 is suitable for measuring leaf movements of larger plant species. Further miniaturization is needed to enable applications of the sensor system for smaller plant species such as Arabidopsis.

Materials and methods

Plant material and abiotic stress treatments

Diurnal and stress-induced leaf movements were assessed in different species and for three major stress conditions (waterlogging, drought, and salinity) in a greenhouse with automated climate control and fertigation supply. The waterlogging treatment started in the morning at 9 AM (1–2 h zeitgeber time) and the high salinity treatment started around 12 AM (4–5 h zeitgeber time). The experiments were conducted under controlled conditions of 18°C and 70% RH during the day and 65% RH during the night and plants received extra assimilation light from 6 AM to 10 PM (SON-T) if solar intensities dropped below 250 W m^{-2}. Waterlogging, drought, and salt treatments were performed on tomato (*S. lycopersicum* cv Ailsa Craig) plants grown in rockwool blocks, after reaching the eighth leaf stage. The waterlogging treatment was conducted by flooding individual containers and lasted for 3 d, after which the plants ($n = 10$) were reoxygenated. For the drought treatment, plants ($n = 4$–8) were subjected to a three-step drying sequence. Initially, plants received water in the morning and the evening for 4 d, followed by only one water gift in the morning. After another 3 d, plants received no fertigation anymore. For the salt stress treatment, plants ($n = 4$) received a sodium chloride-enriched fertigation solution with an electrical conductivity (EC) of 10 dS m^{-1} for 7 d. Control plants received a fertigation solution with an EC of 2.3 dS m^{-1} through drip irrigation at regular time intervals, depending on the solar radiation. To assess circadian leaf movements in tomato, three cultivars were compared while grown in the same greenhouse conditions (*S. lycopersicum* cv Ailsa Craig, cv Severianin, and cv Cuba Plum; $n = 10$). Plant age effects on leaf movements were determined by comparing tomato plants (cv Ailsa Craig) in the seventh and eighth leaf stages ($n = 10$).

Bell pepper (*Capsicum annuum* cv Maduro; $n = 10$) and cucumber (*Cucumis sativus* cv Roxanna; $n = 5$) plants were grown on rockwool in the greenhouse until approximately the seventh leaf stage, after which they received a waterlogging treatment of 3 and 2 d, respectively. Potato (*Solanum tuberosum*) plants were grown from cuttings in a growth room (21°C and 65% RH) until the 13th leaf stage. Afterward, they were transferred to the greenhouse where they received fertigation in the morning and at midday. Subsequently, the potato plants ($n = 9$) received a waterlogging treatment for 3 d. The youngest eight leaves were monitored throughout the experiment. Three lettuce cultivars (*L. sativa* cv Fairly, Lucrecia and Lugano) were grown in rockwool blocks and transferred to a gully system using nutrient film technique (EC 1.7 dS m^{-1}) for 3 weeks. Growth-related leaf movements were monitored for the following 10 d ($n = 4$–6). Common bean (*P. vulgaris* cv Proton) plants were grown in soil pots in the greenhouse until the fifth leaf stage and subsequently exposed to a waterlogging treatment of 5 d by flooding the root system ($n = 10$). For banana, three different crop wild relatives were grown in soil pots in the greenhouse (*M. balbisiana*, *M. acuminata* ssp. *banksii*, and *M. acuminata* ssp. *malaccensis*). Half of the banana plants were subjected to a 4-week drought treatment by withholding irrigation, while the other half was grown under well-watered conditions. Banana was grown under a 12 h/12 h light/dark regime with temperatures between 18°C and 26°C. Maize (*Z. mays*) seedlings ($n = 10$) were grown in soil pots in growth room conditions (21°C and 65% RH) and their growth movements were monitored in time.

Oxygen consumption, transpiration, and salt content (EC) measurements

During each of the waterlogging experiments, the dissolved oxygen level was measured with optical oxygen sensor probes (Firesting O2, Pyroscience) in the container for at least two replicates per species. Drought treatment effects were assessed with continuous lysimeters for the tomato and banana experiments. For the salt stress experiment, the EC in the rockwool blocks of tomato plants was measured with EC-sensors (GS3; Decagon, Pullman, WA, USA).

Leaf and seedling movement

Circadian and stress-induced leaf movements and growth-related seedling movements were assessed with our sensor system (described in the "Results"). Sensors were attached

to the leaf petiole base and stem with flexible clips and to banana leaf laminae with small magnets. Leaf movement was inferred from angular changes of the petiole or the lamina and reported as the respective change of inclination angle.

Validation of the sensor system with image-based analysis was performed on tomato (Ailsa Craig) leaves. Petioles of eight plants at two developmental stages were imaged from the side with individual cameras (Foscam PoE IP camera) and the petiole angle was quantified by image analysis in ImageJ (Schneider et al., 2012). These results were compared with the output of the corresponding leaf angle sensor.

For the maize seedling movements, inclination angles were trigonometrically converted into projected x- and y-coordinates to represent the Cartesian position in a horizontal plane. The trigonometric projection of maize seedling stems was performed using the following conversion:

$$\begin{cases} x = \sin(\theta) * \sin(\psi) \\ y = \sin(\theta) * \cos(\psi) \end{cases},$$

with θ = pitch and ψ = yaw.

Quaternions provide an integrative way of representing these angular features and were compared to top view images for one of the maize plants, by point tracking of an image sequence in ImageJ. Canopy cover of banana plants was determined from weekly top view images starting 4 weeks before the drought treatment. Lettuce canopy cover was determined from images at the start and after 5 d with OpenCV in Python (Bradski, 2000). This pipeline was also used to assess the effect of a waterlogging treatment on the canopy cover of four tomato plants. Images were taken at 10 minute intervals for 6 d.

Data analysis and statistics

Post-processing and visualization of the sensor data were performed in R (R Core Team, 2019), together with the analysis of angular features and plant transpiration. The time series analysis consisted of two main procedures. Data were first interpolated to a common timeframe and the time series were decomposed using seasonal and rrend decomposition using loess (STL decomposition; R packages *tsclean and stl*). In this loess (local regression) based decomposition, outliers of the residual component were removed (values outside the interquartile range times 3). Confidence intervals (90%) were determined from the Student's t-distribution at each time point. Daily leaf angle amplitudes were calculated based on the detrended seasonal (daily) component of the time series, and reported as the difference between the daily maximum and minimum angle. Daily leaf angle changes were calculated as the difference between mean daily leaf angles of the trend component of the time series. Outliers (values outside the interquartile range times 1.5) were removed and distributions were compared using a nonparametric Wilcoxon test in case of a single comparison or a nonparametric Dunn's test following a Kruskal–Wallis test in case of multiple comparisons. Multiple comparisons

were conducted using a Bonferroni correction ($\alpha = 0.05$). Sensor stability was assessed for a number of sensors not attached to leaves, and the total change and daily leaf angle amplitude were calculated using a time series of 1 week and 34 d. Figures were produced using the R package ggplot2 (Wickham, 2016).

Supplemental data

The following materials are available in the online version of this article.

Supplemental Figure S1. Sensor calibration and accuracy.

Supplemental Figure S2. Comparison of steady-state sensor behavior to plant movements.

Supplemental Figure S3. Long-term steady-state sensor stability.

Supplemental Figure S4. Validation of the sensor pitch movement before and during root hypoxia for tomato (Ailsa Craig).

Supplemental Figure S5. Leaf angle amplitudes of the circadian rhythms of leaves of different ages and different tomato accessions.

Supplemental Figure S6. Noncentered data of the circadian leaf movements of different banana genotypes (corresponding to Figure 3C).

Supplemental Figure S7. Oxygen consumption in the root zone of individual plants of different species during a waterlogging treatment.

Supplemental Figure S8. Real-time canopy cover change in Ailsa Craig tomato plants during waterlogging.

Supplemental Figure S9. Average daily leaf angle trend change during control and high salinity conditions in tomato (cv Ailsa Craig) ($n = 4$, EC $= 10$).

Supplemental Figure S10. Daily leaf angle amplitudes of leaves of different ages (fourth, fifth, and sixth leaves) during abiotic stress conditions in tomato (cv Ailsa Craig).

Supplemental Figure S11. Mean hourly transpiration of tomato (cv Ailsa Craig) plants during well-watered conditions and drought stress.

Supplemental Figure S12. Noncentered data of the circadian leaf movements of banana during drought stress (corresponding to Figure 5C).

Supplemental Figure S13. Transpiration of the three banana genotypes during well-watered and water deficit conditions.

Supplemental Figure S14. Comparison of the daily leaf angle changes to waterlogging of tomato and potato.

Supplemental Figure S15. Daily leaf angle amplitudes of different aged leaves and in different species during a waterlogging treatment and recovery.

Supplemental Figure S16. Side- and top-view images of the orientation of a single maize plant during 4 d of growth.

plant propagation and phenotyping, and Kristof Holsteens for his help with the salt stress setup.

Funding

Conflict of interest statement. There is no conflict of interest.

References

Ache P, Bauer H, Kollist H, Al-Rasheid KAS, Lautner S, Hartung W, Hedrich R (2010) Stomatal action directly feeds back on leaf turgor: new insights into the regulation of the plant water status from non-invasive pressure probe measurements. Plant J **62**: 1072–1082

Apelt F, Breuer D, Olas JJ, Annunziata MG, Flis A, Nikoloski Z, Kragler F, Stitt M (2017) Circadian, carbon, and light control of expansion growth and leaf movement. Plant Physiol **174**: 1949–1968

Arana MV, Marín-De La Rosa N, Maloof JN, Blázqueza MA, Alabadí D (2011) Circadian oscillation of gibberellin signaling in Arabidopsis. Proc Natl Acad Sci USA **108**: 9292–9297

Atamian HS, Harmer SL (2016) Circadian regulation of hormone signaling and plant physiology. Plant Mol Biol **91**: 691–702

Bailey-Serres J, Voesenek LACJ (2008) Flooding stress: acclimations and genetic diversity. Ann Rev Plant Biol **59**: 313–339

Baret F, Madec S, Irfan K, Lopez J, Comar A, Hemmerlé M, Dutartre D, Praud S, Tixier MH (2018) Leaf-rolling in maize crops: from leaf scoring to canopy-level measurements for phenotyping. J Exp Bot **69**: 2705–2716

Barmeier G, Schmidhalter U (2017) High-throughput field phenotyping of leaves, leaf sheaths, culms and ears of spring barley cultivars at anthesis and dough ripeness. Front Plant Sci **8**: 1–16

Bastien R, Douady S, Moulia B (2014) A unifying modeling of plant shoot gravitropism with an explicit account of the effects of growth. Front Plant Sci **5**: 1–9

Bastien R, Guayasamin O, Douady S, Moulia B (2018) Coupled ultradian growth and curvature oscillations during gravitropic movement in disturbed wheat coleoptiles. PLoS One **13**: 1–16

Binder BM, O'Malley RC, Wang W, Zutz TC, Bleecker AB (2006) Ethylene stimulates nutations that are dependent on the ETR1 receptor. Plant Physiol **142**: 1690–1700

Biskup B, Scharr H, Schurr U, Rascher U (2007) A stereo imaging system for measuring structural parameters of plant canopies. Plant Cell Environ **30**: 1299–1308

Bours R, Muthuraman M, Bouwmeester H, van der Krol A (2012) OSCILLATOR: a system for analysis of diurnal leaf growth using infrared photography combined with wavelet transformation. Plant Method **8**: 1–12

Bours R, van Zanten M, Pierik R, Bouwmeester H, van der Krol A (2013) Antiphase light and temperature cycles affect PHYTOCHROME B-Controlled ethylene sensitivity and biosynthesis, limiting leaf movement and growth of Arabidopsis. Plant Physiol **163**: 882–895

Bradford KJ, Yang SF (1980) Xylem transport of 1-aminocyclopropane-1-carboxylic acid, an ethylene precursor, in waterlogged tomato plants. Plant Physiol **65**: 322–326

Bradski G (2000) The open CV library. Dr Dobbs Journal of Software Tools.

Briglia N, Williams K, Wu D, Li Y, Tao S, Corke F, Montanaro G, Petrozza A, Amato D, Cellini F et al. (2020) Image-based assessment of drought response in grapevines. Front Plant Sci **11**: 1–12

Cal AJ, Sanciangco M, Rebolledo MC, Luquet D, Torres RO, McNally KL, Henry A (2019) Leaf morphology, rather than plant water status, underlies genetic variation of rice leaf rolling under drought. Plant Cell Environ **42**: 1532–1544

Caldeira CF, Jeanguenin L, Chaumont F, Tardieu F (2014) Circadian rhythms of hydraulic conductance and growth are enhanced by drought and improve plant performance. Nat Commun **5**: 1–9

Chen TW, Nguyen TMN, Kahlen K, Stützel H (2014) Quantification of the effects of architectural traits on dry mass production and light interception of tomato canopy under different temperature regimes using a dynamic functional-structural plant model. J Exp Bot **65**: 6399–6410

Ciszak M, Masi E, Baluška F, Mancuso S (2016) Plant shoots exhibit synchronized oscillatory motions. Commun Integr Biol **9**: e1238117

Clauw P, Coppens F, De Beuf K, Dhondt S, Van Daele T, Maleux K, Storme V, Clement L, Gonzalez N, Inzé D (2015) Leaf responses to mild drought stress in natural variants of Arabidopsis. Plant Physiol **167**: 800–816

de Lucas M, Davière JM, Rodríguez-Falcón M, Pontin M, Iglesias-Pedraz JM, Lorrain S, Fankhauser C, Blázquez MA, Titarenko E, Prat S (2008) A molecular framework for light and gibberellin control of cell elongation. Nature **451**: 480–484

Dieleman JA, De Visser PHB, Meinen E, Grit JG, Dueck TA (2019) Integrating morphological and physiological responses of tomato plants to light quality to the crop level by 3D modeling. Front Plant Sci **10**: 1–12

Disney M, Burt A, Wilkes P, Armston J, Duncanson L (2020) New 3D measurements of large redwood trees for biomass and structure. Sci Rep **10**: 1–11

Dornbusch T, Michaud O, Xenarios I, Fankhauser C (2014) Differentially phased leaf growth and movements in Arabidopsis depend on coordinated circadian and light regulation. Plant Cell **26**: 3911–3921

Dou D, Han S, Cao L, Ku L, Liu H, Su H, Ren Z, Zhang D, Zeng H, Dong Y et al. (2020) CLA4 regulates leaf angle through multiple hormone signaling pathways in maize. J Exp Bot **72**: 1782–1794

Dubois M, Claeys H, Van den Broeck L, Inzé D (2017) Time of day determines Arabidopsis transcriptome and growth dynamics under mild drought. Plant Cell Environ **40**: 180–189

Edelman NF, Jones ML (2014) Evaluating ethylene sensitivity within the family Solanaceae at different developmental stages. HortScience **49**: 628–636

El-iklil Y, Karrou M, Benichou M (2000) Salt stress effect on epinasty in relation to ethylene production and water relations in tomato Salt stress effect on epinasty in relation to ethylene production and water relations in tomato. Agronomie **20**: 399–406

Else MA, Jackson MB (1998) Transport of 1-aminocyclopropane-1-carboxylic acid (ACC) in the transpiration stream of tomato (Lycopersicon esculentum) in relation to foliar ethylene production and petiole epinasty. Austral J Plant Physiol **25**: 453–458

Eyland D, Breton C, Sardos J, Kallow S, Panis B, Swennen R, Paofa J, Tardieu F, Welcker C, Janssens SB et al. (2021) Filling the gaps in gene banks: collecting, characterizing, and phenotyping wild banana relatives of Papua New Guinea. Crop Sci **61**: 137–149

Fahlgren N, Feldman M, Gehan MA, Wilson MS, Shyu C, Bryant DW, Hill ST, McEntee CJ, Warnasooriya SN, Kumar I et al. (2015) A versatile phenotyping system and analytics platform reveals diverse temporal responses to water availability in Setaria. Mol Plant **8**: 1520–1535

Fos M, Nuez F, García-Martínez JL (2000) The gene pat-2, which induces natural parthenocarpy, alters the gibberellin content in unpollinated tomato ovaries. Plant Physiol **122**: 471–479

Gehan MA, Fahlgren N, Abbasi A, Berry JC, Callen ST, Chavez L, Doust AN, Feldman MJ, Gilbert KB, Hodge JG et al. (2017) PlantCV v2: image analysis software for high-throughput plant phenotyping. PeerJ **2017**: 1–23

Golbach F, Kootstra G, Damjanovic S, Otten G, van de Zedde R (2016) Validation of plant part measurements using a 3D reconstruction method suitable for high-throughput seedling phenotyping. Mach Vis Appl **27**: 663–680

Greenham K, Lou P, Remsen SE, Farid H, McClung CR (2015) TRiP: tracking rhythms in plants, an automated leaf movement analysis program for circadian period estimation. Plant Methods **11**: 1–11

Greenham K, McClung CR (2015) Integrating circadian dynamics with physiological processes in plants. Nat Rev Genet **16**: 598–610

Grundy J, Stoker C, Carré IA (2015) Circadian regulation of abiotic stress tolerance in plants. Front Plant Sci **6**: 1–15

Hamant O, Moulia B (2016) How do plants read their own shapes? New Phytol **212**: 333–337

Hartman S, van Dongen N, Renneberg DMHJ, Welschen-Evertman RAM, Kociemba J, Sasidharan R, Voesenek LACJ (2020) Ethylene differentially modulates hypoxia responses and tolerance across Solanum species. Plants **9**: 1022

Hernandez L (2010) Leaf angle and light interception in sunflower (Helianthus annuus L.). Role of the petiole's mechanical and anatomical properties. Phyton **79**: 109–115

Hisamatsu T, King RW, Helliwell CA, Koshioka M (2005) The involvement of gibberellin 20-oxidase genes in phytochrome-regulated petiole elongation of Arabidopsis. Plant Physiol **138**: 1106–1116

Hosoi F, Nakabayashi K, Omasa K (2011) 3-D modeling of tomato canopies using a high-resolution portable scanning lidar for extracting structural information. Sensors **11**: 2166–2174

InvenSense Inc (2016) InvenSense – MPU-6000 and MPU-6050 Product Specification. InvenSense Inc., San Jose, CA

Itakura K, Hosoi F (2019) Estimation of leaf inclination angle in three-dimensional plant images obtained from lidar. Remote Sens **11**: 344

Jackson MB, Campbell DJ (1975) Movement of ethylene from roots to shoots, a factor in the responses of tomato plants to waterlogged soil conditions. New Phytol **74**: 397–406

Jackson MB, Campbell DJ (1976) Waterlogging and petiole epinasty in tomato: the role of ethylene and low oxygen. New Phytol **76**: 21–29

Jin S, Su Y, Wu F, Pang S, Gao S, Hu T, Liu J, Guo Q (2019) Stem-leaf segmentation and phenotypic trait extraction of individual maize using terrestrial LiDAR Data. IEEE Trans Geosci Remote Sens **57**: 1336–1346

Jones RA, El-Beltagy AS (1989) Epinasty promoted by salinity or ethylene is an indicator of salt-sensitivity in tomatoes. Plant Cell Environ **12**: 813–817

Kazemi S, Kefford NP (1974) Apical correlative effects in leaf epinasty of tomato. Plant Physiol **54**: 512–519

Kim H, Kim Y, Yeom M, Lim J, Nam HG (2016) Age-associated circadian period changes in Arabidopsis leaves. J Exp Bot **67**: 2665–2673

Kissel E, van Asten P, Swennen R, Lorenzen J, Carpentier SC (2015) Transpiration efficiency versus growth: exploring the banana biodiversity for drought tolerance. Sci Hortic **185**: 175–182

Koller D, Ritterl S (1996) Light-driven movements of the trifoliate leaves of bean (Phaseolus vulgaris L.). Spectral and functional analysis. J Plant Physiol **149**: 384–392

LemnaTec (2021). Home - lemnatec. https://www.lemnatec.com/ (February 9, 2021)

Levitt J (1986) Recovery of turgor by wilted, excised cabbage leaves in the absence of water uptake. Plant Physiol **82**: 147–153

Lizana C, Wentworth M, Martinez JP, Villegas D, Meneses R, Murchie EH, Pastenes C, Lercari B, Vernieri P, Horton P et al. (2006) Differential adaptation of two varieties of common bean to abiotic stress I. Effects of drought on yield and photosynthesis. J Exp Bot **57**: 685–697

Lynn BH, Carlson TN (1990) A stomatal resistance model illustrating plant vs. external control of transpiration. Agric For Meteorol **52**: 5–43

Mantilla-Perez MB, Salas Fernandez MG (2017) Differential manipulation of leaf angle throughout the canopy: current status and prospects. J Exp Bot **68**: 5699–5717

Marcolino-Gomes J, Rodrigues FA, Fuganti-Pagliarini R, Bendix C, Nakayama TJ, Celaya B, Molinari HBC, De Oliveira MCN, Harmon FG, Nepomuceno A (2014) Diurnal oscillations of soybean circadian clock and drought responsive genes. PLoS One **9**: e86402

McClung CR (2006) Plant circadian rhythms. Plant Cell **18**: 792–803

Moulia B, Bastien R, Chauvet-Thiry H, Leblanc-Fournier N (2019) Posture control in land plants: Growth, position sensing, proprioception, balance, and elasticity. J Exp Bot **70**: 3467–3494

Mullen JL, Weinig C, Hangarter RP (2006) Shade avoidance and the regulation of leaf inclination in Arabidopsis. Plant Cell Environ **29**: 1099–1106

Müller-Linow M, Pinto-Espinosa F, Scharr H, Rascher U (2015) The leaf angle distribution of natural plant populations: assessing the canopy with a novel software tool. Plant Methods **11**: 1–16

Müller NA, Jiménez-Gómez JM (2016) Analysis of circadian leaf movements. In P Duque, ed, Environmental Responses in Plants: Methods and Protocols, Springer New York, New York, NY, pp 71–79

Müller NA, Wijnen CL, Srinivasan A, Ryngajllo M, Ofner I, Lin T, Ranjan A, West D, Maloof JN, Sinha NR et al. (2015) Domestication selected for deceleration of the circadian clock in cultivated tomato. Nat Genet **48**: 89–93

Müller NA, Zhang L, Koornneef M, Jiménez-Gómez JM (2018) Mutations in EID1 and LNK2 caused light-conditional clock deceleration during tomato domestication. Proc Natl Acad Sci USA **115**: 7135–7140

Nagano S, Moriyuki S, Wakamori K, Mineno H, Fukuda H (2019) Leaf-movement-based growth prediction model using optical flow analysis and machine learning in plant factory. Front Plant Sci **10**: 1–10

Naito H, Ogawa S, Valencia MO, Mohri H, Urano Y, Hosoi F, Shimizu Y, Chavez AL, Ishitani M, Selvaraj MG, Omasa K (2017) Estimating rice yield related traits and quantitative trait loci analysis under different nitrogen treatments using a simple tower-based field phenotyping system with modified single-lens reflex cameras. ISPRS J Photogramm Remote Sens **125**: 50–62

Pantazopoulou CK, Bongers FJ, Küpers JJ, Reinen E, Das D, Evers JB, Anten NPR, Pierik R (2017) Neighbor detection at the leaf tip adaptively regulates upward leaf movement through spatial auxin dynamics. Proc Natl Acad Sci USA **114**: 7450–7455

Papadopoulos AP, Pararajasingham S (1997) The influence of plant spacing on light interception and use in greenhouse tomato (Lycopersicon esculentum Mill.): a review. Sci Hortic **69**: 1–29

Paproki A, Sirault X, Berry S, Furbank R, Fripp J (2012) A novel mesh processing based technique for 3D plant analysis. BMC Plant Biol **12**: 1–13

Park YJ, Lee HJ, Gil KE, Kim JY, Lee JH, Lee H, Cho HT, Vu LD, Smet I, De Park CM (2019) Developmental programming of thermonastic leaf movement. Plant Physiol **180**: 1185–1197

Pastenes C, Pimentel P, Lillo J (2005) Leaf movements and photoinhibition in relation to water stress in field-grown beans. J Exp Bot **56**: 425–433

Perrier X, De Langhe E, Donohue M, Lentfer C, Vrydaghs L, Bakry F, Carreel F, Hippolyte I, Horry JP, Jenny C et al. (2011) Multidisciplinary perspectives on (Musa spp.) domestication. Proc Natl Acad Sci USA **108**: 11311–11318

Phenospex (2021) Smart plant analysis & phenotyping systems. https://phenospex.com/ (January 20, 2021)

Polko JK, van Zanten M, van Rooij JA, Marée AFM, Voesenek LACJ, Peeters AJM, Pierik R (2012) Ethylene-induced differential petiole growth in *Arabidopsis thaliana* involves local microtubule reorientation and cell expansion. New Phytol **193**: 339–348

Polko JK, Voesenek LACJ, Peeters AJM, Pierik R (2011) Petiole hyponasty: an ethylene-driven, adaptive response to changes in the environment. AoB Plants **11**: 1–11

R Core Team (2019) R: a language and environment for statistical computing. R Foundation for Statistical Computing, Vienna, Austria

Rankenberg T, Geldhof B, van Veen H, Holsteens K, Van de Poel B, Sasidharan R (2021) Age-dependent abiotic stress resilience in plants. Trend Plant Sci **26**: 1–14

Rauf M, Arif M, Fisahn J, Xue GP, Balazadeh S, Mueller-Roeber B (2013) NAC transcription factor SPEEDY HYPONASTIC GROWTH regulates flooding-induced leaf movement in Arabidopsis. Plant Cell **25**: 4941–4955

Riviere M, Derr J, Douady S (2017) Motions of leaves and stems, from growth to potential use. Phys Biol **14**: 051001

Ruiz-Sánchez MC, Domingo R, Torrecillas A, Pérez-Pastor A (2000) Water stress preconditioning to improve drought resistance in young apricot plants. Plant Sci **156**: 245–251

Salter MG, Franklin KA, Whitelam GC (2003) Gating of the rapid shade-avoidance response by the circadian clock in plants. Nature **426**: 680–683

Sarlikioti V, De Visser PHB, Marcelis LFM (2011) Exploring the spatial distribution of light interception and photosynthesis of canopies by means of a functionalstructural plant model. Ann Bot **107**: 875–883

Sasidharan R, Hartman S, Liu Z, Martopawiro S, Sajeev N, van Veen H, Yeung E, Voesenek LACJ (2017) Signal dynamics and interactions during flooding stress. Plant Physiol **176**: 1106–1117

Schneider CA, Rasband WS, Eliceiri KW (2012) NIH Image to ImageJ: 25 years of image analysis. Nat Methods **9**: 671–675

Schrager-Lavelle A, Gath NN, Devisetty UK, Carrera E, López-Díaz I, Blázquez MA, Maloof JN (2019) The role of a class III gibberellin 2-oxidase in tomato internode elongation. Plant J **97**: 603–615

Shi W, van de Zedde R, Jiang H, Kootstra G (2019) Plant-part segmentation using deep learning and multi-view vision. Biosyst Eng **187**: 81–95

Sisodia R, Bhatla SC (2018) Plant movements. *In* Plant Physiology, Development and Metabolism, Vol. **192**, Springer Singapore, Singapore, pp 907–935

Smeets ME, Voesenek LACJ, Peeters AJM, Benschop JJ, Millenaar FF, van Zanten M (2006) Abscisic acid antagonizes ethylene-induced hyponastic growth in Arabidopsis. Plant Physiol **143**: 1013–1023

Smith M, Ullberg D (1989) Effect of leaf angle and orientation on photosynthesis and water relations in Silphium terebinthinaceum. Am J Bot **76**: 1714–1719

Stevens B, Diels J, Vanuytrecht E, Brown A, Bayo S, Rujweka A, Richard E, Ndakidemi PA, Swennen R (2020) Canopy cover evolution, diurnal patterns and leaf area index relationships in a Mchare and Cavendish banana cultivar under different soil moisture regimes. Sci Hortic **272**: 109328

Su W, Zhu D, Huang J, Guo H (2018) Estimation of the vertical leaf area profile of corn (*Zea mays*) plants using terrestrial laser scanning (TLS). Comput Electron Agric **150**: 5–13

Thain SC, Vandenbussche F, Laarhoven LJJ, Dowson-Day MJ, Wang ZY, Tobin EM, Harren FJM, Millar AJ, Van Der Straeten D (2004) Circadian rhythms of ethylene emission in Arabidopsis. Plant Physiol **136**: 3751–3761

Thapa S, Zhu F, Walia H, Yu H, Ge Y (2018) A novel LiDAR-Based instrument for high-throughput, 3D measurement of morphological traits in maize and sorghum. Sensors **18**: 1187

Thomas DS, Turner DW (2001) Banana (Musa sp.) leaf gas exchange and chlorophyll fluorescence in response to soil drought, shading and lamina folding. Sci Hortic **90**: 93–108

Tseng T-S, Salomé PA, McClung CR, Olszewski NE (2004) SPINDLY and GIGANTEA interact and act in Arabidopsis thaliana pathways involved in light responses, flowering, and rhythms in cotyledon movements. Plant cell **16**: 1550–1563

Van Wesemael J, Hueber Y, Kissel E, Campos N, Swennen R, Carpentier S (2018) Homeolog expression analysis in an allotriploid non-model crop via integration of transcriptomics and proteomics. Sci Rep **8**: 1–11

van Zanten M, Ritsema T, Polko JK, Leon-Reyes A, Voesenek LACJ, Millenaar FF, Pieterse CMJ, Peeters AJM (2012) Modulation of ethylene- and heat-controlled hyponastic leaf movement in *Arabidopsis thaliana* by the plant defence hormones jasmonate and salicylate. Planta **235**: 677–685

Vandenbrink JP, Brown EA, Harmer SL, Blackman BK (2014) Turning heads: the biology of solar tracking in sunflower. Plant Sci **224**: 20–26

Verma A, Niranjana M, Jha SK, Mallick N, Agarwal P, Vinod (2020) QTL detection and putative candidate gene prediction for leaf rolling under moisture stress condition in wheat. Sci Rep **10**: 1–13

Wang X, Zhang R, Song W, Han L, Liu X, Sun X, Luo M, Chen K, Zhang Y, Yang H et al. (2019) Dynamic plant height QTL revealed in maize through remote sensing phenotyping using a high-throughput unmanned aerial vehicle (UAV). Sci Rep **9**: 1–10

Weisz PR, Randall HC, Sinclair TR (1989) Water relations of turgor recovery and restiffening of wilted cabbage leaves in the absence of water uptake. Plant Physiol **91**: 433–439

Wickham H (2016) ggplot2: Elegant Graphics for Data Analysis. Berlin, Germany: Springer Science & Business Media

Wieser M, Puttonen E, Mandlburger G, Zlinszky A, Briese C, Pfeifer N, Pfennigbauer M (2016) Quantification of overnight movement of birch (*Betula pendula*) branches and foliage with short interval terrestrial laser scanning. Front Plant Sci **7**: 1–13

WIWAM (2019) Automated systems for plant phenotyping – WIWAM presents phenotyping platforms for plant phenotype analysis. https://www.wiwam.be/ (January 20, 2021)

Zhang J, Ku LX, Han ZP, Guo SL, Liu HJ, Zhang ZZ, Cao LR, Cui XJ, Chen YH (2014) The ZmCLA4 gene in the qLA4-1 QTL controls leaf angle in maize (*Zea mays* L.) J Exp Bot **65**: 5063–5076